


## ORIGINAL ARTICLE

# Circulating exosomal microRNAs as diagnostic and prognostic biomarkers in patients with diffuse large B-cell lymphoma

Di Cao<sup>1</sup>  | Xia Cao<sup>1</sup> | Yu Jiang<sup>1,2</sup> | Juan Xu<sup>1</sup> | Yuhuan Zheng<sup>1</sup> | Deying Kang<sup>3</sup> | Caigang Xu<sup>1</sup>

<sup>1</sup>Department of Hematology, West China Hospital, Sichuan University, Chengdu, China

<sup>2</sup>Department of Hematology, The Affiliated Hospital of Yunnan University, Kunming, China

<sup>3</sup>Department of Evidence-Based Medicine and Clinical Epidemiology, Sichuan University, Chengdu, China

## Correspondence

Caigang Xu, Department of Hematology, West China Hospital, Sichuan University, Chengdu 610041, China.

Email: [xucaigang@yahoo.com](mailto:xucaigang@yahoo.com)

## Funding information

Sichuan Science and Technology Department, Grant/Award Number: 2019YFS0027

## Abstract

Exosomal microRNAs (miRNAs) are potential biomarkers for a variety of tumors, but have not yet been studied in diffuse large B-cell lymphoma (DLBCL). Here, we investigated the use of exosomal miRNAs in DLBCL diagnosis and prognosis. A total of 256 individuals, including 133 DLBCL patients, 94 healthy controls (HCs), and 29 non-DLBCL concurrent controls (CCs), were enrolled. Exosomal miRNAs were profiled in the screening stage using microarray analysis, and miRNA candidates were confirmed in training, testing, and external testing stages using qRT-PCR. Follow-up information on the DLBCL patients was collected, and miRNAs were used to develop diagnostic and prognostic models for these patients. Five exosomal miRNAs (miR-379-5p, miR-135a-3p, miR-4476, miR-483-3p, and miR-451a) were differentially expressed between DLBCL patients and HCs with areas under the receiver operating characteristic curve (AUC) of 0.86, 0.90, and 0.86 for the training, testing, and external testing stages, respectively. Four exosomal miRNAs (miR-379-5p, miR-135a-3p, miR-4476, and miR-451a) were differentially expressed between patients with DLBCL and CCs, with an AUC of 0.78. One miRNA (miR-451a) was significantly associated with both progression-free survival (PFS) and overall survival (OS) of DLBCL patients, R analysis indicated the combination of miR-451a with international prognostic index was a better predictor of PFS and OS for these patients. Our study suggests that subsets of circulating exosomal miRNAs can be useful noninvasive biomarkers for the diagnosis of DLBCL and that the use of circulating exosomal miRNAs improves the identification of patients with newly diagnosed DLBCL with poor outcomes.

## KEYWORDS

diagnosis, diffuse large B-cell lymphoma, exosome, microRNA, prognosis

This is an open access article under the terms of the Creative Commons Attribution-NonCommercial-NoDerivs License, which permits use and distribution in any medium, provided the original work is properly cited, the use is non-commercial and no modifications or adaptations are made.

© 2021 The Authors. Hematological Oncology published by John Wiley & Sons Ltd.

## 1 | INTRODUCTION

Diffuse large B-cell lymphoma (DLBCL) is a lymphoproliferative disorder that originates in B-lymphocytes. As the most common subtype of non-Hodgkin lymphoma (NHL), it accounts for 30%–40% of all NHL globally<sup>1</sup> and for more than 15,000 deaths in China every year.<sup>2</sup> Currently, the diagnosis of DLBCL depends largely on pathologic analysis of biopsy tissue,<sup>3</sup> which is an invasive procedure and poses risks to patients. In addition, although the international prognostic index (IPI) has been widely used as a prognostic factor for DLBCL cases,<sup>4</sup> patients in similar prognostic groups often have heterogeneous outcomes,<sup>5</sup> suggesting certain shortcomings with the current prognostic evaluation system.

Exosomes are tiny vesicles (30–100 nm in diameter) wrapped in cup-shaped lipid bilayers that are released into body fluids by many types of cells.<sup>6</sup> Exosomes are stable in peripheral blood and encapsulate many bioactive molecules,<sup>6,7</sup> such as signal proteins, enzymes, and nucleic acids, including microRNAs (miRNAs).<sup>6</sup> These miRNAs are small (21–23 nucleotides), noncoding RNAs that help regulate gene expression through interaction with mRNA at the post-transcriptional level.<sup>8</sup> Several studies have suggested that exosomal miRNAs isolated from peripheral blood can be noninvasive biomarkers for detecting tumors or monitoring disease progression and treatment efficacy.<sup>9–11</sup> However, their value in assessing patients with DLBCL has not yet been determined.

Here, we conducted a study consisting of five sequential stages to determine the value of exosomal miRNAs in DLBCL (Figure 1). In the screening stage, we identified 22 exosomal miRNAs that were significantly differentially expressed between DLBCL cases and healthy controls using an Exiqon microarray platform. In the training stage, we winnowed the 22 exosomal miRNAs to 5 miRNAs using quantitative reverse transcription polymerase chain reaction (qRT-PCR). These five exosomal miRNAs were further confirmed in the cohort of testing and external testing stages using qRT-PCR. Finally, we evaluated the 5-miRNA panel's diagnostic performance with logistic regression and prognostic performance using the R-language. Our results indicated that the 5-miRNA panel showed an excellent performance in diagnosing DLBCL, and the combined "IPI + miR-451a" model performed better than IPI or miR-451a data alone in predicting the outcomes of DLBCL patients.

## 2 | METHODS

Figure 1 shows the flow chart of the study.

### 2.1 | Participants

The cohort in the screening stage included 10 DLBCL patients and 5 HCs, with no significant age or sex difference between the two groups. We further interrogated a training stage of 48 individuals, a testing stage of 164 individuals, and an external testing stage of 241

individuals. The three stages were as follows: cohort (1) in the training stage included 24 DLBCL patients and 24 HCs; (2) in the testing stage consisting of 99 DLBCL patients and 65 HCs, and (3) in the external testing stage included 123 DLBCL patients, 89 HCs, and 29 non-DLBCL concurrent controls (CCs). 123 DLBCL patients and 89 HCs in external testing stage were recruited from the training and testing stages; 29 CCs were patients who had 1 of 3 lymphoma subtypes, including 19 natural killer/T-cell lymphoma cases, 4 follicular lymphoma cases, and 6 Hodgkin lymphoma cases.

Healthy controls were people whose health status was confirmed by routine physical examinations at West China Hospital. Hospitalized patients with lymphoma were recruited at the Department of Hematology and Department of Oncology in West China Hospital who did not receive any specific treatment (including surgical treatment, chemotherapy, or radiotherapy) without other malignancies or serious infections between December 2016 and May 2018. The diagnosis of lymphoma was established using the National Comprehensive Cancer Center guideline.<sup>12</sup> Post-treatment surveillance evaluation was conducted through outpatient follow-up or telephone interviews every 3 months for the first year and every 6 months for the next few years. The cutoff date for follow-up was 31 October 2020.

This study was approved by the Institutional Review Board of West China Hospital (No. 2016 (302)). All participants provided written informed consent for blood collection and follow-up.

### 2.2 | Exosome isolation and characterization

A 6-ml peripheral blood sample was collected from each participant within 48 h of admission and separated for serum within 4 h. Exo-Quick Exosome Precipitation Solution (System Biosciences), an isolation kit for sensitive downstream application,<sup>9</sup> was used to extract exosomes from serum (Figure S1A). Isolated exosomes were identified by nanoparticle tracking analysis (NTA), transmission electron microscopy (TEM), and western blotting. Specifically, the size and concentration of particles were examined by NTA using a Nanosight NS300 (Malvern Instruments). The morphology of particles was determined using TEM (FEI Tecnai™ G2 Spirit) at 80 kV. The exosome-specific marker proteins CD63, CD81, and HSP70 were detected by western blot and probed with corresponding antibodies (System Biosciences). GAPDH (Beyotime) was used as an internal control.

### 2.3 | Exosomal RNA isolation and cDNA preparation

Total RNA was extracted using the miRNeasy Serum/Plasma Advanced Kit (Qiagen) according to the manufacturer's instructions. Ce\_miR-39\_1 (Qiagen) was chosen as a "spike-in" normalization control for qRT-PCR quantification<sup>13,14</sup> and added to the reaction system when exosome pellets were resuspended in

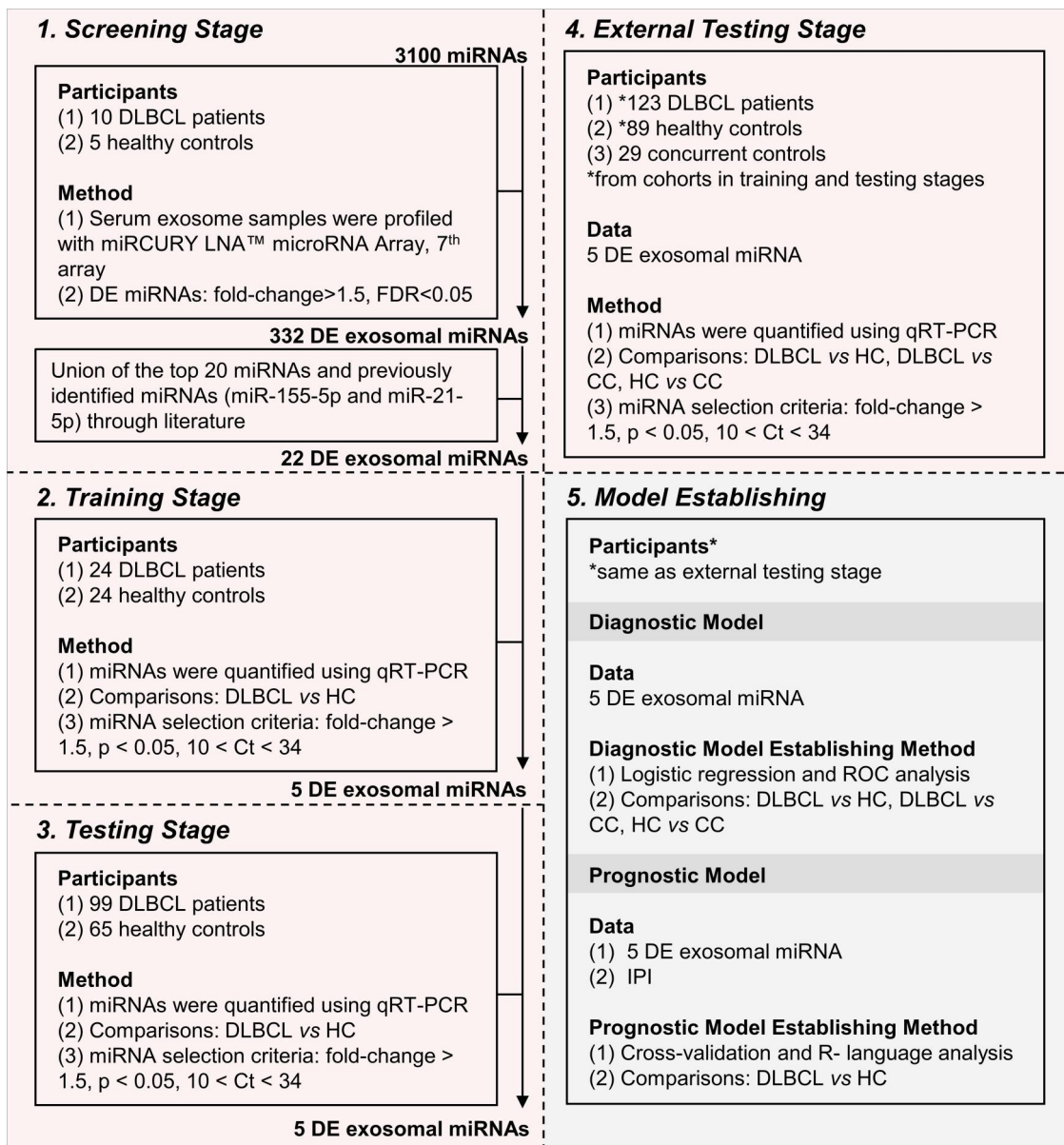


**FIGURE 1** Overview of the strategy for investigating exosomal miRNAs and diagnostic and prognostic models for DLBCL patients. CC, concurrent control; DE exosomal miRNAs, differentially expressed exosomal miRNAs; DLBCL, diffuse large B-cell lymphoma; HC, healthy control; IPI, international prognostic index

Qiazol. RNA quality and yield were measured using an ND-1000 Nanodrop Spectrophotometer (Thermo Fisher Scientific). RNA samples with a 260/280-nm absorbance ratio greater than 1.8 and a 260/230-nm absorbance ratio greater than 2.0 were considered acceptable for subsequent analysis. A miScript II RT Kit (Qiagen) was used to reverse transcribe the cDNA. The obtained cDNA was diluted in 100  $\mu$ l of RNase-free water and stored at  $-80^{\circ}\text{C}$  until further use.

## 2.4 | Exosomal RNA profiling

RNA labeling and array hybridization were performed by Kang-Chen Bio-Tech Company according to the manufacturer's

instructions. Replicated miRNAs were averaged, and miRNAs with intensities  $\geq 30$  in all samples were chosen for calculating the normalization factor. Expressed data were normalized using median normalization, and differentially expressed exosomal miRNAs with statistical significance were selected based on the following criteria: an absolute expression fold change greater than 1.5 and a false discovery rate value less than 0.05. Real-time PCR was performed to confirm the conformation. Differentially expressed miRNAs were identified using volcano plot screening. Cluster analysis was carried out by hierarchical clustering to show distinguishable miRNA expression profiles among samples. The microarray profile data were submitted to the NCBI Gene Expression Omnibus (GSE171272, <https://www.ncbi.nlm.nih.gov/geo/query/acc.cgi?acc=GSE171272>).

## 2.5 | miRNA qRT-PCR quantification

MiRNA was quantified using the miScript SYBR<sup>®</sup> Green PCR Kit and miRNA-specific primers (Qiagen). A no-cDNA template control and a negative control were included in each plate. All miRNAs were measured in a blinded fashion, and all samples were analyzed in triplicate. The average cycle threshold (Ct) was recorded. The  $Ct_{(miRNA)}$  had to range between 10 and 34 to be acceptable. The relative concentration of miRNA was calculated using the comparative  $2^{-\Delta\Delta Ct}$  method as follows:  $\Delta Ct = Ct_{(miRNA)} - Ct_{(Ce\_miR-39\_1)}$  and  $\Delta\Delta Ct = \Delta Ct - \text{average } Ct_{(healthy\ control)}$ .

## 2.6 | Statistical methods

Nonparametric Mann–Whitney or Kruskal–Wallis tests were used to compare relative miRNA expression levels between different groups; Kaplan–Meier method and log-rank test were applied to plot progression-free survival (PFS) and overall survival (OS); Cox proportional hazard model was employed to identify independent outcome predictor and compute hazard ratio; receiver operating characteristic (ROC) curve and logistic regression were adopted to estimate the diagnostic value of the candidate miRNAs.

Predictive value of the “miRNA + IPI” model for PFS and OS was calculated with R language and a *K*-fold cross-validation method was applied to avoid overfitting.<sup>9,15</sup> In brief, data were first split into *K* folds:  $F_1, F_2, \dots, F_k$  (parameter *K* = 5 in this process). For *i* in 1, ..., *K*, we used one fold  $F_i$  as the validation set, then the other *K* – 1 folds as the training set to build the Cox model, and *coxph* function in survival package was applied to fit the Cox model. Finally, AUC of this model on the validation set was evaluated and the calculation formula of AUC was  $AUC = \frac{1}{K} \sum_{i=1}^K AUC_i$ .

Data were analyzed using SPSS v22.0, GraphPad Prism v7.0, and R v3.6.2. All statistical tests were two-sided, alpha was set to 0.05, and 95% confidence intervals (CI) were calculated as needed.

## 3 | RESULTS

### 3.1 | Characteristics of enrolled participants

We prospectively enrolled 256 individuals, including 15 subjects (10 DLBCL patients and 5 HCs) in the screening stage, 48 subjects (24 DLBCL patients and 24 HCs) in the training stage, 164 subjects (99 DLBCL patients and 65 HCs) in the testing stage, and 29 non-DLBCL lymphoma cases who served as concurrent controls in the external testing stage at West China Hospital, Sichuan University. The characteristics of the 256 participants are presented in Table S1.

The median follow-up time of DLBCL cases was 36 months (1–45 months). Of the 123 patients with DLBCL (10 DLBCL patients in the screening stage were excluded to avoid repeated detection), 12 DLBCL patients were lost to follow-up, and another 2 were transferred to local hospitals where the disease state could

not be determined clearly. Finally, 111 DLBCL cases were included for OS analysis, and 109 DLBCL cases were included for PFS analysis.

### 3.2 | Exosome characterization

Nanoparticle tracking and electron microscopy showed that exosomes appeared as cup-shaped vesicles between 80 and 95 nm in diameter (Figure S1B,C), which was consistent with the finding of previous studies.<sup>6,16</sup> Immunoblot analysis detected the exosomal marker proteins CD63, CD81, and HSP70 in the extract (Figure S1D).

### 3.3 | Circulating exosomal miRNA profiling from the screening stage

Among the 3100 miRNAs detected by microarray analysis, 157 were highly expressed and 175 were expressed at low levels in the DLBCL group. The top 20 out of the 332 miRNAs that met the criteria for fold change and statistical significance (Figure 2) with two other miRNAs, miR-155-5p and miR-21-5p,<sup>17,18</sup> which were identified in tissue samples as diagnostic biomarkers for DLBCL by many previous studies, were chosen for the further validation stage outlined below.

### 3.4 | Validation of circulating exosomal miRNAs by qRT-PCR

Expression levels of the 22 miRNAs identified in the screening stage were evaluated in a larger training sample set including 24 DLBCL patients and 24 HCs. As a result, eight individual miRNAs (miR-379-5p, miR-135a-3p, miR-4476, miR-483-3p, miR-451a, miR-551a, miR-135b-5p, and miR-155-5p) that met the predetermined criteria ( $Ct_{(miRNA)}$  values ranging from 10 to 34) were identified and included in the next analysis. Five miRNAs, consisting of three high-expression miRNAs (miR-379-5p, miR-135a-3p and miR-4476) and two low-expression miRNAs (miR-483-3p and miR-451a), among the above eight miRNAs, were differentially expressed, as defined by fold changes greater than 1.5 and *p*-values less than 0.05 (Figure S2A).

Next, these five miRNAs were subjected to validation in the testing stage with 99 DLBCL patients and 65 HCs, and the differential expression patterns of the five miRNAs between DLBCL patients and HCs were concordant with results in the training stage (Figure S2B).

These five miRNAs were subsequently tested in 29 concurrent controls in the external testing stage to assess their potential form in non-DLBCL lymphoma subtype cases. The results suggested that miR-379-5p, miR-135a-3p, miR-4476, and miR-451a were differentially expressed in non-DLBCL lymphoma subtype when compared with those in DLBCL patients, whereas only miR-451a was differentially expressed in on-DLBCL lymphoma subtype when compared with that in HCs (Figure S2C).

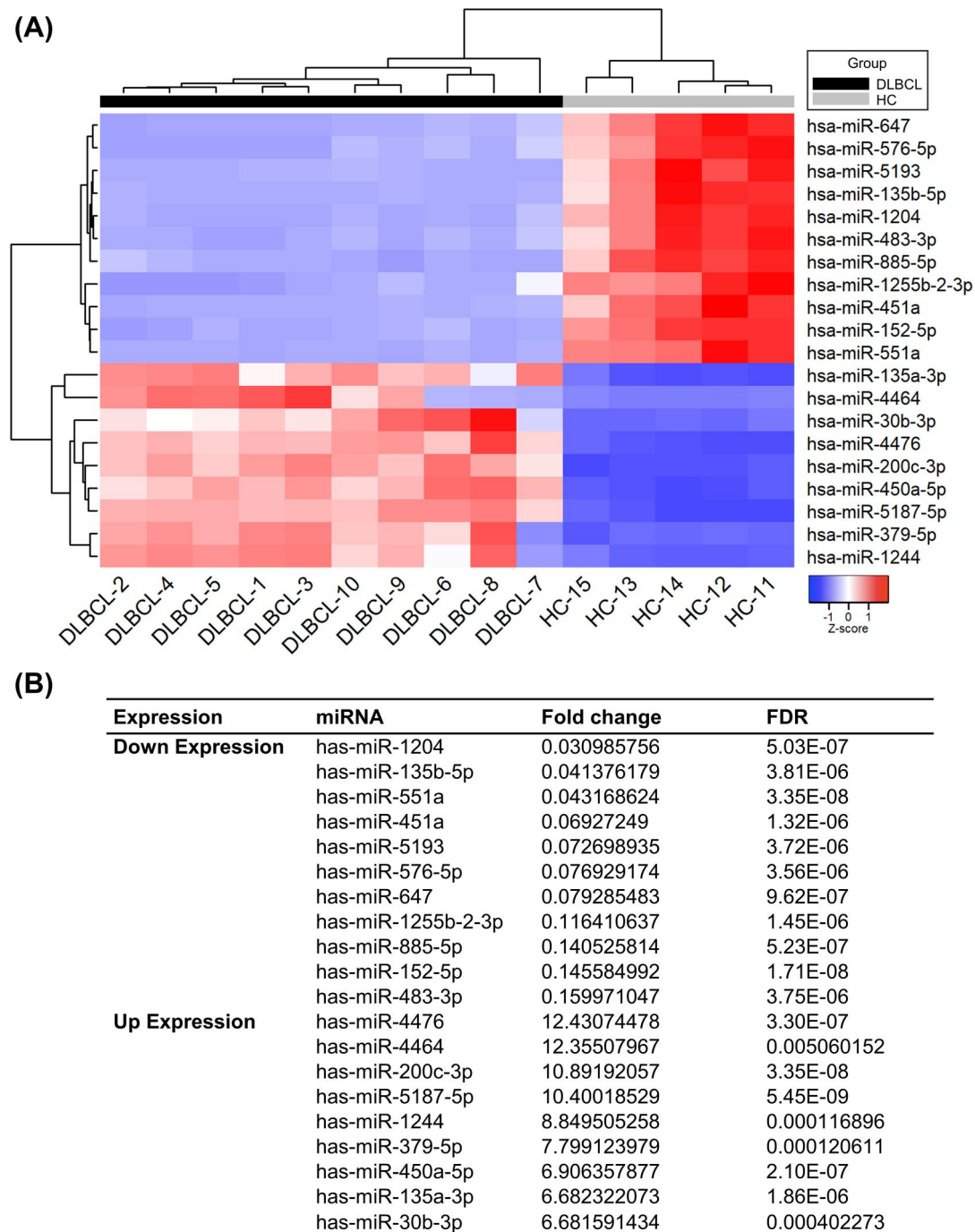


**FIGURE 2** Twenty candidates differentially expressed miRNAs were selected from the screening stage. (A) Hierarchical clustering of the differentiation between diffuse large B-cell lymphoma (DLBCL) patients and healthy controls based on the expression of 20 differentially expressed exosomal miRNAs. The screening set included 10 DLBCL patients and 5 healthy controls. A red diamond indicates increased miRNA expression, a blue diamond represents decreased miRNA expression, and deeper color means a larger fold change. (B) The expression of 20 miRNAs in the screening stage. FDR, false discovery rate

### 3.5 | Diagnostic value of circulating exosomal miRNAs

To determine the diagnostic performance characteristics of the five miRNAs in distinguishing DLBCL patients from HCs, we plotted ROC curves for each miRNA as well as the 5-miRNA panel in the training, testing, and external testing stages, respectively. The results

suggested that the combined panel of five miRNAs showed better performance in diagnosing DLBCL than a single miRNA signature (Figure 3 and Table 1).

We also plotted ROC curves for the four miRNAs with differential expression between DLBCL patients and lymphoma subtype controls to assess their differential diagnostic ability, and the AUC for miR-379-5p was 0.73 (95% CI: 0.65–0.80; sensitivity: 0.52; specificity:

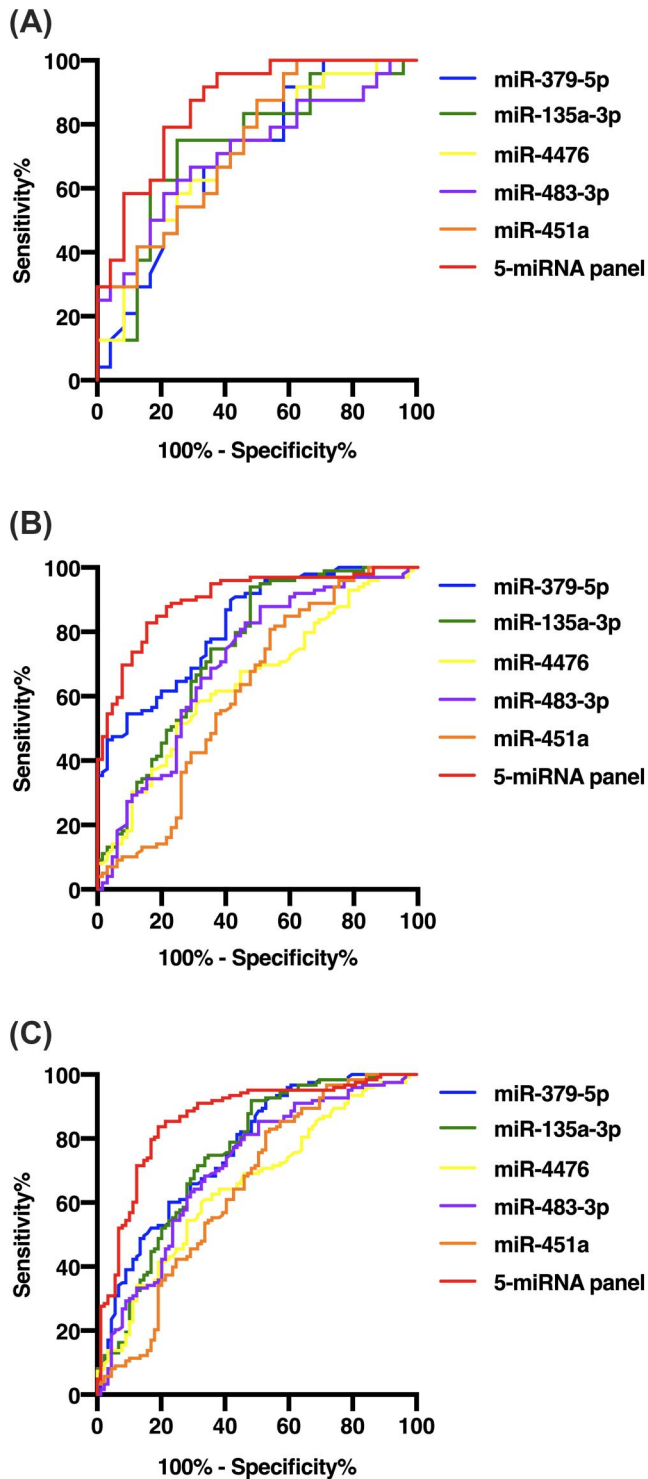


**FIGURE 3** Performance characteristics of circulating exosomal miRNAs in diagnosing diffuse large B-cell lymphoma (DLBCL). Panels A, B, and C show ROC curves of individual miRNAs and the combined miRNA panel in the training, testing, and external testing stages to discriminate DLBCL patients from healthy controls. The AUC of miR-379-5p, miR-135a-3p, miR-4476, miR-483-3p, miR-451a, and the 5-miRNA panel are expressed as blue, green, yellow, purple, orange, and red curves, respectively. (A) Results for 24 DLBCL patients and 24 healthy controls in the training stage. (B) Results for 99 DLBCL patients and 65 healthy controls in the testing stage. (C) Results for 123 DLBCL patients and 89 healthy controls (the combined two cohorts of training and testing stages) in the external testing stage. AUC, area under the curve

0.94); for miR-135a-3p, 0.67 (95% CI: 0.59–0.74; sensitivity: 0.62; specificity: 0.66); for miR-4476, 0.64 (95% CI: 0.55–0.71; sensitivity: 0.31; specificity: 0.98); for miR-451a, 0.67 (95% CI: 0.59–0.75; sensitivity: 0.86; specificity: 0.45); and for 4-miRNA-panel, 0.78 (95% CI: 0.70–0.84; sensitivity: 0.90; specificity: 0.56) (Figure S3A). We subsequently estimated the diagnostic value of miR-451a in distinguishing lymphoma subtype controls from healthy controls. Unexpectedly, miR-451a alone showed excellent performance with an AUC of 0.77 (95% CI: 0.68–0.84; sensitivity: 0.86; specificity: 0.63) (Figure S3B).

### 3.6 | Association between exosomal miRNA abundance and clinical characteristics

To explore the relationship between exosomal miRNA expression levels and clinical parameters, we analyzed clinicopathological correlations in patients with DLBCL, who constituted the largest group included in this study. Our result suggested in DLBCL cohort, adverse prognostic factor of advanced stage disease (stages III–IV) was associated with lower concentrations of miR-451a (Figure S4E).

### 3.7 | Prognostic significance of circulating exosomal miRNAs in DLBCL

Given that exosomal miR-451a was differentially expressed in different DLBCL groups, we hypothesized that these miRNAs may predict the prognosis of DLBCL. We first investigated the association between miRNAs and patient outcomes with miRNA expression dichotomized at the median value. The result showed only miR-451a was a significant risk factor for both of PFS and OS (Figure 4). Moreover, miR-451a was still significant after adjustment for the IPI (Table S2), which is an accepted prognostic factor in DLBCL and also showed excellent performance in predicting outcomes in our DLBCL cohort (Figure S5).

To further assess the prognostic value of the signature of miR-451a, we performed an AUC analysis with cross-validation. The combination of the signature of miR-451a with IPI had better prediction for PFS and OS than when the miR-451a signature was excluded (Figure 5). Together, these data indicated that circulating exosomal miRNAs could improve the prognostic stratification of patients with DLBCL, in addition to the IPI.

## 4 | DISCUSSION

Among various biomolecules associated with tumors, exosomal miRNA is considered as the most promising one. Exosomal miRNAs can be relatively easily isolated from body fluids and tested by qRT-PCR, suggesting their potential roles in cancer diagnosis and prognosis.<sup>9,11,19,20</sup> Compared with other noninvasive biomarkers, exosomal miRNAs have a protective lipid bilayer membrane and are therefore more stable.<sup>13,21,22</sup> In addition, other noninvasive biomarkers may complicate diagnosis and prognosis because they are

TABLE 1 Performance characteristics of microRNAs for diagnostic model in DLBCL patients

miRNA	Training stage			Testing stage			External testing stage		
	AUC (95% CI)	Sensitivity	Specificity	AUC (95% CI)	Sensitivity	Specificity	AUC (95% CI)	Sensitivity	Specificity
miR-379-5p	0.70 (0.55–0.82)	0.75	0.58	0.82 (0.75–0.88)	0.90	0.58	0.77 (0.70–0.82)	0.92	0.47
miR-135a-3p	0.73 (0.59–0.85)	0.75	0.75	0.75 (0.67–0.81)	0.94	0.52	0.75 (0.69–0.81)	0.92	0.52
miR-4476	0.71 (0.56–0.83)	0.50	0.83	0.65 (0.57–0.72)	0.52	0.75	0.65 (0.59–0.72)	0.60	0.67
miR-483-3p	0.71 (0.57–0.84)	0.58	0.79	0.70 (0.63–0.77)	0.88	0.49	0.71 (0.65–0.77)	0.81	0.54
miR-451a	0.74 (0.59–0.85)	0.88	0.50	0.61 (0.53–0.69)	0.81	0.46	0.65 (0.58–0.71)	0.82	0.47
5-miRNA panel	0.86 (0.73–0.94)	0.88	0.71	0.90 (0.85–0.94)	0.83	0.85	0.86 (0.81–0.91)	0.84	0.81

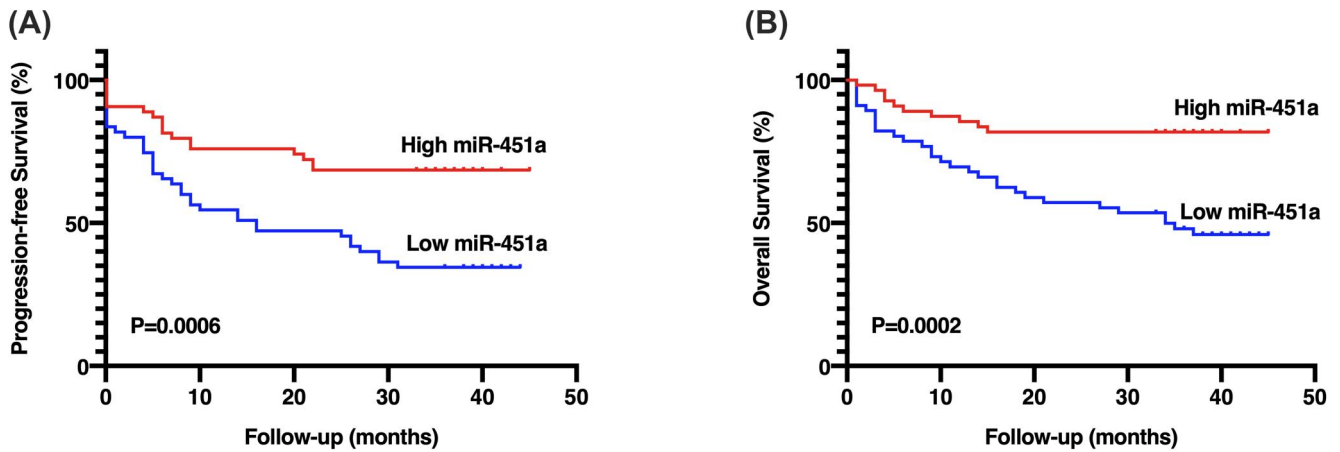


FIGURE 4 Survival analysis of different concentrations of circulating exosomal miR-451a in DLBCL patients. Kaplan-Meier survival curves of (A) predicting progression-free survival and (B) overall survival in patients with DLBCL. miRNAs expression is dichotomized as high or low according to the median value

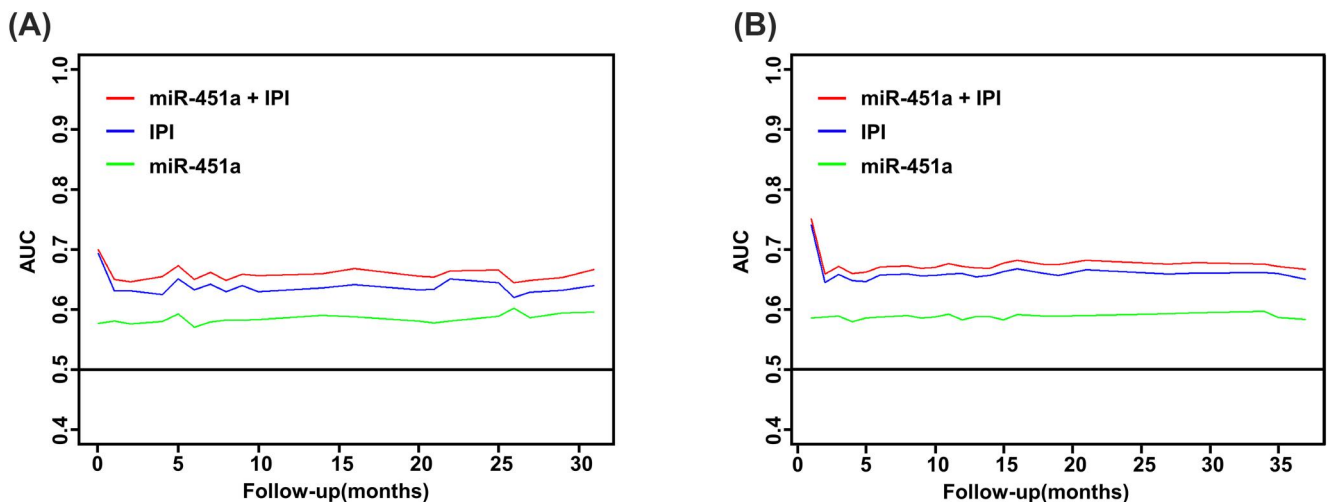


FIGURE 5 Area under the ROC (AUC) curves based on multivariate Cox proportional hazard model using a time-dependent ROC analysis. The AUC of international prognostic index, miR-451a, and the combined indicator miR-451a and IPI are expressed as blue, green, and red curves, respectively. (A) is that for progression-free survival, and (B) is that for overall survival. Cross-validation has been applied to this analysis to avoid overfitting

passively released by apoptotic and necrotic cells.<sup>23</sup> Exosomes, however, are actively secreted by living cells,<sup>10,24</sup> rendering a more reliable body status for predicting diagnosis or prognosis.

In this study, we designed a rigorous five-stage study to determine the value of serum exosomal miRNAs in DLBCL, and five miRNAs (miR-379-5p, miR-135a-3p, miR-4476, miR-483-3p, and miR-

451a) were identified using microarray analysis and qRT-PCR. The combined panel of all five miRNAs had the ability to diagnose DLBCL with an AUC of 0.86. However, the panel did not perform well in discriminating between patients with DLBCL and concurrent controls with lymphoma subtypes. We speculated that this poor ability was principally caused by the complex composition of concurrent controls, which consisted of patients with three different lymphoma subtypes.

Moreover, we found specific circulating exosomal miRNA can be critical in defining worse prognosis in patients with newly diagnosed DLBCL, and combination of miRNA with IPI, an established prognostic factor, could serve as a better indicator for predicting outcomes of these patients. We assumed this improved performance in prognosis was due to the addition of biological heterogeneity of miRNA, remedying shortcomings of the IPI that primarily relies on clinical features. Besides IPI, we also tried to combine miRNA with other potential prognostic factors, like cell-of-origin (COO) classification. However, COO failed to stratify patients' outcomes in our DLBCL cohort (Figure S6), suggesting the prognostic role of COO defined by immunohistochemistry may be still controversial in DLBCL patients.

Even reports regarding these five miRNAs in DLBCL is rare, miRNA-target gene analysis has showed their strong association with DLBCL's generation and development (Figure S7). Studies in other types of tumors also confirmed their roles in cancer pathogenesis and progression. For example, a lower concentration of miR-451a was reported to be associated with a poorer pathologic stage in patients with lung cancer and promoted cell survival by targeting c-MYC in patients with prostate cancer.<sup>25,26</sup> Our previous research also indicated that miR-451a was a potential biomarker for therapy response monitoring in DLBCL patients, and its expression level gradually increased in patients who achieved remission,<sup>27</sup> this result being validated by other researchers.<sup>28</sup> miR-483-5p has been identified as an antitumor miRNA in breast cancer that targets histone deacetylase 8 or cyclin E1, which suggests that miR-483-3p affects cell growth and apoptosis.<sup>29,30</sup>

miR-379-5p has been reported to be downregulated in many cancer tissues. However, overexpression of miR-379-5p was observed in patients with DLBCL in our study. We assumed this because miRNAs could be selectively secreted from original cancer cells by exosomes. A previous study has indicated that miR-379-5p was downregulated in gastric cancer tissue samples and functioned as a tumor suppressor in cancer development. Interestingly, researchers also found that exosomal miR-379-5p was higher in circulating exosomal samples from gastric cancer patients with poor outcomes. Scholars further validated the upregulated expression level of miR-379-5p in a cell line model and speculated that the translocation of miR-379-5p from cancer cells to the circulation system might contribute to the high regulation of miR-379-5p in circulatory exosomal samples.<sup>31</sup> Similar conditions have also been reported in lung cancer.<sup>32,33</sup> This implies that the profiling of miRNAs in circulating exosomes is significantly different from that in tissue or blood.

Both miR-135a-3p and miR-4476 were reported to be upregulated miRNAs that promote cell proliferation, migration, and invasion in CNS tumors.<sup>34,35</sup> Further mechanistic analyses indicated that adenomatous polyposis coli, a negative regulator of the Wnt/ $\beta$ -catenin signaling pathway, is a direct target of miR-4476 and mediates the oncogenic effect of miR-4476 in glioma.<sup>35</sup> This may explain high concentrations of these two miRNAs in DLBCL cases.

## 5 | CONCLUSIONS

In conclusion, we identified a panel of five miRNAs in circulating exosomes that can be used as noninvasive biomarkers for diagnosing DLBCL. Circulating exosomal miR-451a had prognostic value, and the combination of miR-451a with IPI could serve as a better indicator for the prediction of PFS and OS in these patients.

## ACKNOWLEDGMENTS

We thank the staffs of the Hematology Research Laboratory, West China Hospital, for their assistance with this study. We also appreciate the support from Department of Hematology, Oncology, and Laboratory Medicine at West China Hospital. This work was supported by a grant from Sichuan Science and Technology Department to Caigang Xu, MD (No. 2019YFS0027).

## CONFLICT OF INTEREST

The authors have no conflicts of interest to declare that are relevant to the content of this article.

## DATA AVAILABILITY STATEMENT

The data that support the findings of this study are available in GEO at <https://www.ncbi.nlm.nih.gov/geo/query/acc.cgi?acc=GSE171272>.

## ORCID

Di Cao  <https://orcid.org/0000-0002-1205-1556>

## PEER REVIEW

The peer review history for this article is available at <https://publons.com/publon/10.1002/hon.2956>.

## REFERENCES

1. Campo E, Swerdlow SH, Harris NL, Pileri S, Stein H, Jaffe ES. The 2008 WHO classification of lymphoid neoplasms and beyond: evolving concepts and practical applications. *Blood*. 2011;117(19):5019-5032. <https://doi.org/10.1182/blood-2011-01-293050>
2. Chen W, Zheng R, Baade PD, et al. Cancer statistics in China, 2015. *CA Cancer J Clin*. 2016;66(2):115-132. <https://doi.org/10.3322/caac.21338>
3. Liu Y, Barta SK. Diffuse large B-cell lymphoma: 2019 update on diagnosis, risk stratification, and treatment. *Am J Hematol*. 2019;94(5):604-616. <https://doi.org/10.1002/ajh.25460>
4. International Non-Hodgkin's Lymphoma Prognostic Factors P. A predictive model for aggressive non-Hodgkin's lymphoma. *N Engl J*



- Med.* 1993;329(14):987-994. <https://doi.org/10.1056/NEJM19930303291402>
5. Gisselbrecht C, Glass B, Mounier N, et al. Salvage regimens with autologous transplantation for relapsed large B-cell lymphoma in the rituximab era. *J Clin Oncol.* 2010;28(27):4184-4190. <https://doi.org/10.1200/JCO.2010.28.1618>
  6. Thery C, Zitvogel L, Amigorena S. Exosomes: composition, biogenesis and function. *Nat Rev Immunol.* 2002;2(8):569-579. <https://doi.org/10.1038/nri855>
  7. Boukouris S, Mathivanan S. Exosomes in bodily fluids are a highly stable resource of disease biomarkers. *Proteomics Clin Appl.* 2015;9(3-4):358-367. <https://doi.org/10.1002/prca.201400114>
  8. Kong YW, Ferland-McCollough D, Jackson TJ, Bushell M. microRNAs in cancer management. *Lancet Oncol.* 2012;13(6):e249-e258. [https://doi.org/10.1016/s1470-2045\(12\)70073-6](https://doi.org/10.1016/s1470-2045(12)70073-6)
  9. Manier S, Liu CJ, Avet-Loiseau H, et al. Prognostic role of circulating exosomal miRNAs in multiple myeloma. *Blood.* 2017;129(17):2429-2436. <https://doi.org/10.1182/blood-2016-09-742296>
  10. Melo SA, Sugimoto H, O'Connell JT, et al. Cancer exosomes perform cell-independent microRNA biogenesis and promote tumorigenesis. *Cancer Cell.* 2014;26(5):707-721. <https://doi.org/10.1016/j.ccell.2014.09.005>
  11. van Eijndhoven MA, Zijlstra JM, Groenewegen NJ, et al. Plasma vesicle miRNAs for therapy response monitoring in Hodgkin lymphoma patients. *JCI Insight.* 2016;1(19):e89631. <https://doi.org/10.1172/jci.insight.89631>
  12. Zelenetz AD, Gordon LI, Wierda WG, et al. Diffuse large B-cell lymphoma. Version 1.2016. *J Natl Compr Canc Netw.* 2016;14(2):196-231. <https://doi.org/10.6004/jnccn.2016.0023>
  13. Hosokawa K, Kajigaya S, Feng X, et al. A plasma microRNA signature as a biomarker for acquired aplastic anemia. *Haematologica.* 2017;102(1):69-78. <https://doi.org/10.3324/haematol.2016.151076>
  14. Farina NH, Wood ME, Perrapato SD, et al. Standardizing analysis of circulating microRNA: clinical and biological relevance. *J Cell Biochem.* 2014;115(5):805-811. <https://doi.org/10.1002/jcb.24745>
  15. Heagerty PJ, Zheng Y. Survival model predictive accuracy and ROC curves. *Biometrics.* 2005;61(1):92-105. <https://doi.org/10.1111/j.0006-341X.2005.030814.x>
  16. Huang X, Yuan T, Tschannen M, et al. Characterization of human plasma-derived exosomal RNAs by deep sequencing. *BMC Genom.* 2013;14:319. <https://doi.org/10.1186/1471-2164-14-319>
  17. Lim EL, Trinh DL, Scott DW, et al. Comprehensive miRNA sequence analysis reveals survival differences in diffuse large B-cell lymphoma patients. *Genome Biol.* 2015;16(1):18. <https://doi.org/10.1186/s13059-014-0568-y>
  18. Lawrie CH, Soneji S, Marafioti T, et al. MicroRNA expression distinguishes between germinal center B cell-like and activated B cell-like subtypes of diffuse large B cell lymphoma. *Int J Cancer.* 2007;121(5):1156-1161. <https://doi.org/10.1002/ijc.22800>
  19. Lai X, Wang M, McElyea SD, Sherman S, House M, Korc M. A microRNA signature in circulating exosomes is superior to exosomal glypican-1 levels for diagnosing pancreatic cancer. *Cancer Lett.* 2017;393:86-93. <https://doi.org/10.1016/j.canlet.2017.02.019>
  20. Melo SA, Luecke LB, Kahlert C, et al. Glypican-1 identifies cancer exosomes and detects early pancreatic cancer. *Nature.* 2015;523(7559):177-182. <https://doi.org/10.1038/nature14581>
  21. Malumbres R, Sarosiek KA, Cubedo E, et al. Differentiation stage-specific expression of microRNAs in B lymphocytes and diffuse large B-cell lymphomas. *Blood.* 2009;113(16):3754-3764. <https://doi.org/10.1182/blood-2008-10-184077>
  22. Li M, Jia Y, Xu J, Cheng X, Xu C. Assessment of the circulating cell-free DNA marker association with diagnosis and prognostic prediction in patients with lymphoma: a single-center experience. *Ann Hematol.* 2017;96(8):1343-1351. <https://doi.org/10.1007/s00277-017-3043-5>
  23. Mohrmann L, Huang H, Hong DS, et al. Liquid biopsies using plasma exosomal nucleic acids and plasma cell-free DNA compared with clinical outcomes of patients with advanced cancers. *Clin Cancer Res.* 2017;24:181-188. <https://doi.org/10.1158/1078-0432.ccr-17-2007>
  24. Taylor DD, Gercel-Taylor C. MicroRNA signatures of tumor-derived exosomes as diagnostic biomarkers of ovarian cancer. *Gynecol Oncol.* 2008;110(1):13-21. <https://doi.org/10.1016/j.ygyno.2008.04.033>
  25. Chen Q, Hu H, Jiao D, et al. miR-126-3p and miR-451a correlate with clinicopathological features of lung adenocarcinoma: the underlying molecular mechanisms. *Oncol Rep.* 2016;36(2):909-917. <https://doi.org/10.3892/or.2016.4854>
  26. Chang C, Liu J, He W, et al. A regulatory circuit HP1gamma/miR-451a/c-Myc promotes prostate cancer progression. *Oncogene.* 2017;37:415-426. <https://doi.org/10.1038/onc.2017.332>
  27. Cao D, Jiang Y, Feng Y, Jing CX, Xu J, Xu CG. [The value of circulating exosomal miR-451a to monitor therapy response in diffuse large B cell lymphoma]. *Sichuan da Xue Xue Bao Yi Xue Ban [J Sichuan Univ Med Sci Ed.]* 2018;49(3):399-403.
  28. Xiao XB, Gu Y, Sun DL, et al. Effect of rituximab combined with chemotherapy on the expression of serum exosome miR-451a in patients with diffuse large b-cell lymphoma. *Eur Rev Med Pharmacol Sci.* 2019;23(4):1620-1625. [https://doi.org/10.26355/eurrev\\_2019\\_02\\_17121](https://doi.org/10.26355/eurrev_2019_02_17121)
  29. Huang X, Lyu J. Tumor suppressor function of miR-483-3p on breast cancer via targeting of the cyclin E1 gene. *Exp Ther Med.* 2018;16(3):2615-2620. <https://doi.org/10.3892/etm.2018.6504>
  30. Menbari MN, Rahimi K, Ahmadi A, et al. miR-483-3p suppresses the proliferation and progression of human triple negative breast cancer cells by targeting the HDAC8>oncogene. *J Cell Physiol.* 2020;235(3):2631-2642. <https://doi.org/10.1002/jcp.29167>
  31. Liu X, Chu KM. Exosomal miRNAs as circulating biomarkers for prediction of development of haematogenous metastasis after surgery for stage II/III gastric cancer. *J Cell Mol Med.* 2020;24(11):6220-6232. <https://doi.org/10.1111/jcmm.15253>
  32. Zhou F, Nie L, Feng D, Guo S, Luo R. MicroRNA-379 acts as a tumor suppressor in non-small cell lung cancer by targeting the IGF-1R-mediated AKT and ERK pathways. *Oncol Rep.* 2017;38(3):1857-1866. <https://doi.org/10.3892/or.2017.5835>
  33. Cazzoli R, Buttitta F, Di Nicola M, et al. microRNAs derived from circulating exosomes as noninvasive biomarkers for screening and diagnosing lung cancer. *J Thorac Oncol.* 2013;8(9):1156-1162. <https://doi.org/10.1097/JTO.0b013e318299ac32>
  34. Cipro Š, Belhajová M, Eckschlager T, Zámečník J. MicroRNA expression in pediatric intracranial ependymomas and their potential value for tumor grading. *Oncol Lett. Jan.* 2019;17(1):1379-1383. <https://doi.org/10.3892/ol.2018.9685>
  35. Lin J, Ding S, Xie C, et al. MicroRNA-4476 promotes glioma progression through a miR-4476/APC/β-catenin/c-Jun positive feedback loop. *Cell Death Dis.* 2020;11(4):269. <https://doi.org/10.1038/s41419-020-2474-4>

## SUPPORTING INFORMATION

Additional supporting information may be found in the online version of the article at the publisher's website.

**How to cite this article:** Cao D, Cao X, Jiang Y, et al.

Circulating exosomal microRNAs as diagnostic and prognostic biomarkers in patients with diffuse large B-cell lymphoma. *Hematol Oncol.* 2022;40(2):172-180. <https://doi.org/10.1002/hon.2956>